

A Redshift Survey in Quasar Fields

Our previous extensive imaging surveys of quasar fields (e.g., Yee and Green 1987, Ellingson, Yee and Green 1991) have shown that the properties and evolution of active galactic nuclei (AGN) are intimately connected with their galaxy cluster environment. We found that quasars in rich galaxy clusters evolve 5-6 times faster than their counterparts in poorer environments. This rapid evolution of AGN activity in rich clusters is responsible for the result that at $z > 0.5$ the brightest radio-loud quasars are often found in rich clusters of galaxies; whereas, at the present epoch, clusters host only objects with very faint AGN activity (e.g. DeRobertis and Yee 1990).

The rapid evolution of radio-loud AGN in rich environments is most likely to be tied to the evolution of the physical conditions within the cluster core. Timescales for the evolution of the AGN activity are similar to dynamical timescales for these clusters, consistent with this scenario. One possible physical mechanism which may drive the evolution of AGN on these timescales is dynamical evolution of the cluster core. In this scenario, the virialization of the cluster core raises the velocities of galaxies in the core to the point where galaxy-galaxy interactions are no longer efficient enough to trigger AGN activity (e.g. Roos 1985). Our previous preliminary spectroscopic study of galaxies associated with bright quasars carried out at KPNO indicates that the velocity dispersions of these environments are low, in agreement with this model (Ellingson, Green and Yee 1991). A second scenario is that a dense intra-cluster medium strips galaxies in the cluster core, depriving the AGN of one source of gaseous fuel.

To investigate the dynamics and gas content of galaxies in the quasar environment and their effect on AGN activity, we are currently carrying out a redshift survey of galaxies in fields of quasars previously identified as being situated in rich clusters. Two other important studies are also being carried out using the same database. First, the majority of galaxies in this study are actually foreground and background galaxies. These objects can be used as a pencil-beam redshift survey for the study of galaxy evolution in the field and for the study of large scale

structure. Second, the combination of the presence of a reasonably bright quasar in the centers of these fields and the extensive redshift data of foreground galaxies makes these data useful in the study of quasar absorption lines, and the properties of Lyman α and metal absorption systems.

The MARLIN focal reducer and LAMA aperture mask system were used to obtain both deep images and multi-object spectroscopy of faint galaxies in fields surrounding quasars.

To date, we have obtained data in 7 quasar fields in three runs in 1991 and 1992 in which we had about 6 usable nights. The sample consists of radio-loud quasars with $0.3 < z < 0.6$, which were found to be situated in clusters of Abell richness class 1 or greater. At the start of each run, direct images in Gunn r and g were obtained for each of the fields to be observed using MARLIN in direct imaging mode. These images were reduced and analyzed in real time at the summit. They were debiassed and flatfielded using IRAF, and processed using the object finding, classification and photometry program PPP (Yee 1991). From the list of galaxies in these images, candidates for spectroscopy were chosen based on star-galaxy classification and magnitude, usually in the range of $19 < r < 22$. The brighter limit was chosen to preferentially select objects at redshifts similar to the quasar, and the fainter limit to assure that an absorption-line redshift could be determined with spectroscopic integration times of 2-3 hours. Multi-slit aperture masks were designed using the interactive graphics software available at the summit. The slit width was chosen to be 2" in order to gather as much light from the extended galaxies as possible in the event that flexure or other alignment problems misplaced the object, and the minimum slit length was set to be 10" to ensure adequate accuracy in the background sky subtraction. Each mask included 25 to 30 objects. The aperture masks were then fabricated using the LAMA laser. The first mask of the run usually required about 1.5-2 hours to design and fabricate, while simultaneously taking direct images of the other target fields so as to make the most efficient use of telescope time. Subsequent mask were created during the rest of the first night, and often the next afternoon.

The multi-object spectra were reduced using the *msred* package in IRAF (see Ellingson, 1989 for details). We use a

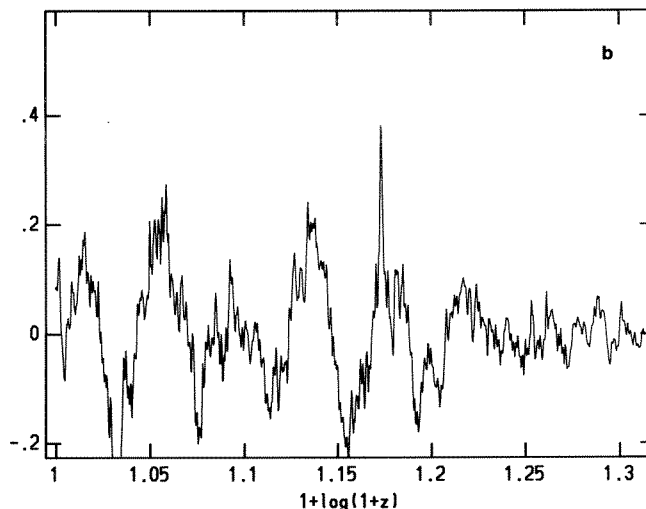
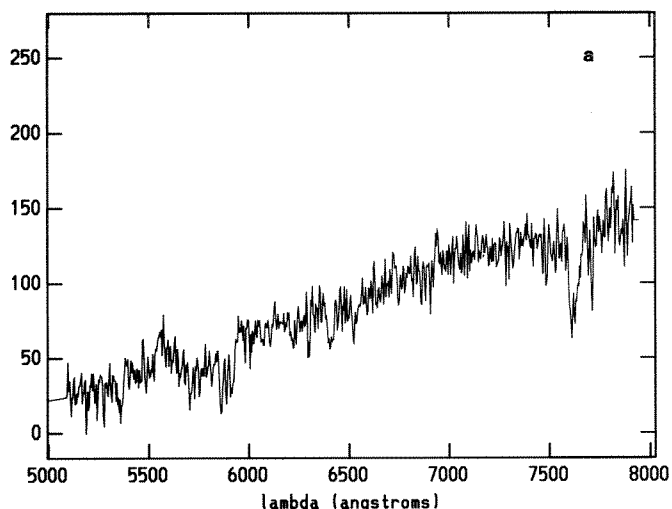


Figure 17: Spectra and correlations of faint galaxies. Figures a and b show the spectrum and correlation function for a galaxy with $r = 21.83$

and $z = 0.4896$. The correlation peak has $R = 4.2$.

cross-correlation technique (see Ellingson and Yee 1992) to determine redshifts of low-signal-noise spectra of absorption-line galaxies. Extensive simulations of realistic galaxy spectra have been used to determine the statistical confidence level of redshift identifications made by this method. Figure 17 shows examples of data and correlation functions. The confidence parameter R has been tested by extensive simulations of realistic galaxy spectra. Identifications with $R=3.5$ are found to be confident at better than the 90% level. In general, only redshifts identified by correlations with $R > 3.5$, or clearly identified by emission lines are used.

From these data we have determined redshifts for 208 galaxies, 61 of which are associated with the quasars. We were able to determine a redshift for 81% of targeted galaxies with $r < 21.5$ mag, and 71% for those with $r < 22.2$ mag. Some of the spectra are unidentified spectra due to defocussing on one side of the field. In a 4×6 arcminute field centered on each quasar, this sample is currently 48% complete for all objects brighter than 21.5 mag in the 7 fields.

Figure 18 shows the distribution of galaxies in our sample as a function of Gunn $g-r$ color and redshift. Objects with

absorption and emission line redshifts are marked. Also plotted are non-evolving K-corrected colors of galaxies of different morphological types at different redshifts. The color and emission-line characteristics of the data are entirely consistent with the models. Note the decrease in the fraction of emission line objects with increasing redshift, which is probably due to the difficulties of determining absorption line redshifts for the fainter objects.

Velocity cluster dispersion around the quasar redshift were calculated for individual clusters based on 5 to 20 cluster member velocities. In a preliminary analysis, velocity dispersions of individual were found to agree with the scenario discussed above, where increasing velocity dispersions are accompanied by a decrease in the optical AGN activity. While a definitive correlation between quasar activity and cluster dynamics awaits a more complete dataset, these results suggest that galaxy-galaxy interactions are important in the triggering or fueling of quasar activity.

Several fields show remarkable structures in redshift space. Figure 19 wedge diagrams of the fields surrounding 3C 215, a quasar at $z = 0.411$. In this figure, emission line galaxies are

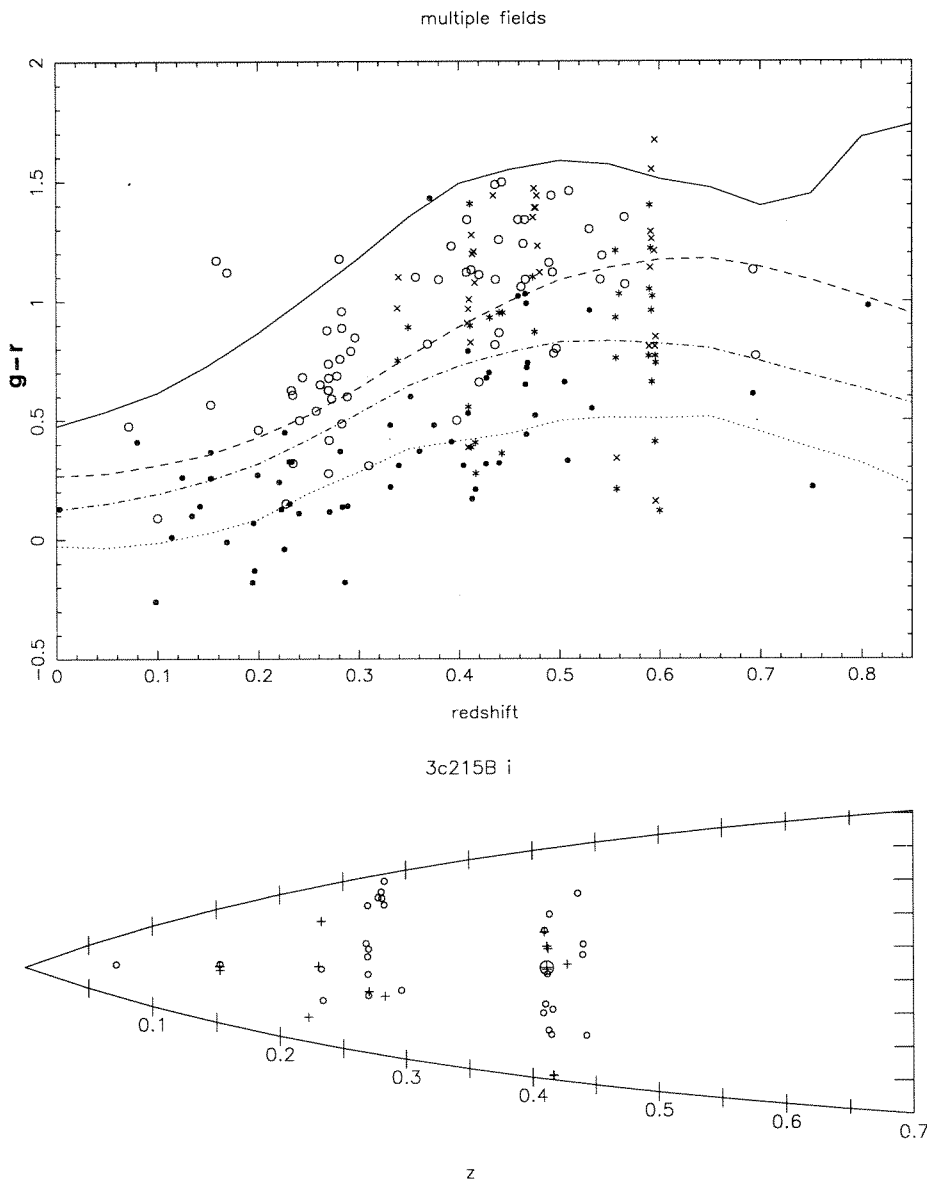


Figure 18: The distribution of $g-r$ versus z for galaxies in our sample. Open dots denote absorption-line field galaxies, and crosses denote absorption-line galaxies associated with quasars. Solid dots denote emission line field galaxies and stars denote emission line galaxies associated with quasars. Also plotted are non-evolving K-corrected colors of galaxies of different morphological types at different redshifts.

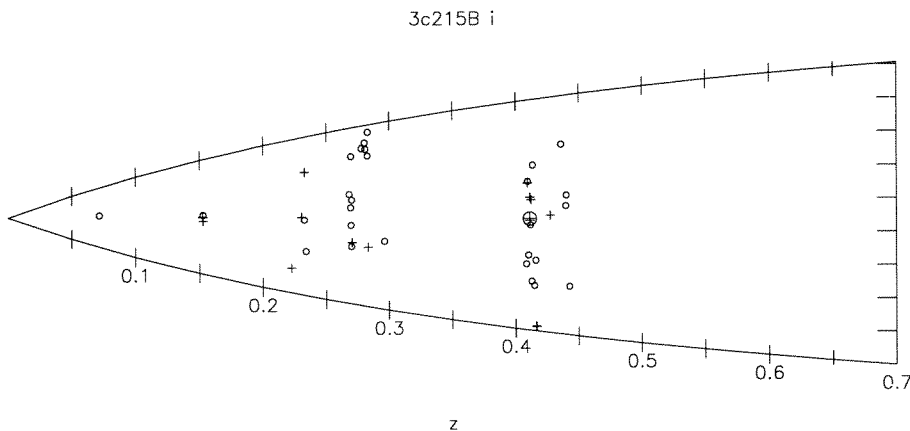


Figure 19: Wedge diagram for the field surrounding the quasar 3C 215 at $z = 0.411$. Open dots are absorption line galaxies, and crosses are emission line galaxies. Tick marks on the vertical axis are 0.25 Mpc, apart, giving an aspect ratio of about 1500.

marked by crosses and absorption line galaxies by open dots. Note that there are at least three "sheets" of galaxies in this field in addition to the cluster associated with the quasar. We also found that although the field surrounding the quasar 1641 + 399 at $z = 0.59$ does not seem to contain a cluster of galaxies centered on the quasar, it does show a remarkably rich structure with a large number of emission line galaxies. Given that the quasar 3C 345, located 8 arcminutes away at the same redshift, also has several galaxies associated with it, this area may contain a very large and rich sheet of galaxies.

Finally, a fairly large number of galaxies in these fields are close enough to the quasar line-of-sight so that absorptions in the quasar spectra can be correlated with galaxy redshifts. The incidence of Mg II absorption from galaxies with known redshifts has been investigated by Bechtold and Ellingson (1992), and we are collaborating with members of the Hubble Space Telescope Key Project, who have taken ultraviolet spectra of several of our objects. A number of correlations have been found, which will be used to interpret the nature of metal and Lyman α absorptions also seen at higher redshifts. It is clear that these observations represent an important and necessary complement to the study of these systems.

*E. Ellingson, University of Colorado
H.K.C. Yee, University of Toronto*

References

- Bechtold, J. and Ellingson, E. 1992, *ApJ*, in press.
 DeRobertis, M. and Yee, H.K.C. 1990 *AJ*, **100**, 84.
 Ellingson, E., 1989, "A User's Guide to Multi-object Spectroscopic Reduction with IRAF", NOAO manual.
 Ellingson, E., Green, R.F., & Yee, H.K.C., 1991, *ApJ*, **378**, 476.
 Ellingson, E., and Yee, H.K.C., 1992, *AJ*, in preparation.
 Ellingson, E., and Yee, H.K.C., and Green, R.F., 1991, *ApJ*, **371**, 36.
 Roos, N. 1985 *A&A*, **104**, 218.
 Yee, H.K.C., 1991, *AJ*, **103**, 396.
 Yee, H.K.C. and Ellingson, E., 1992, *ApJ*, submitted.
 Yee, H.K.C. and Green, R.F. 1987, *ApJ*, **319**, 28. (YG87)

Magnetospheres of Helium-Peculiar Stars

Nonthermal phenomena have been known to occur in the environments of massive main sequence stars for several years. Many O stars show evidence of variable nonthermal radio emission, as well as variable soft x-ray emission, and in spite of the relatively homogeneous nature of O stars there is a wide range of radio or x-ray luminosity for a given bolometric luminosity. In addition, the UV spectra of O stars and the cooler Be stars have lines of superionized species that can only be present in plasma much hotter than the photospheric temperatures of these stars. Apparently some source of nonradiative energy and momentum is needed in the winds of most, or all OB stars. The transfer of energy from surface magnetic fields via magnetohydrodynamic waves is one possibility, and a number of investigators have also considered the possibility that the winds from massive stars are influenced directly by stellar magnetic fields. Since the winds from these stars contribute as much energy and momentum to the interstellar medium as do supernovae a firm understanding of the importance of such nonthermal processes is of widespread interest.

To date, magnetic fields have not been directly detected in the majority of hot stars showing evidence of stellar winds. This does not mean that such fields do not exist, as they could be below current detection limits or have geometries that make detection difficult with conventional polarimetric techniques. Fortunately, globally ordered magnetic fields have been known to exist in many members of the various classes of chemically peculiar stars for almost fifty years. The hottest of these, the helium-peculiar stars, include the approximately two dozen B2-B3 helium-strong stars which have neutral helium lines too strong for their colours, and the larger group of B3 - late B helium-weak stars with abnormally weak helium lines. Both classes are spectroscopic and photometric variables, have large (> 1 kG), variable longitudinal magnetic fields, and have magnetically controlled stellar winds as demonstrated by variable UV resonance lines of CIV and SiIV. A few have also been established as non-thermal radio sources, and possibly radio variables. The helium-peculiar stars therefore display many of the same phenomena seen in massive OB stars and provide us with excellent laboratories for investigating the importance of magnetically controlled winds and magnetospheres in hot stars.

The oblique rotator model provides a satisfactory conceptual picture for understanding the observations of the helium-peculiar stars. A magnetic field (generally dipolar) inclined to the rotation axis interacts with diffusion processes as well as the stellar wind. The result is a non-uniform surface abundance consisting of belts or spots usually roughly axisymmetric with the magnetic axis. However, because of the tilt of the magnetic axis the abundance geometry is not symmetrical with respect to the rotation axis and spectrum variations, as well as photometric variations, occur on the rotation period of the star, typically a few days. The helium abundance peculiarities arise because of competition between the gravitational settling of helium and the general outflow in the stellar wind. Above the surface, the magnetic field also exerts a strong influence by trapping some of the stellar wind in a stellar magnetosphere, forming co-rotating clouds of plasma several stellar radii above the photosphere. These circumstellar clouds are the source of the H α emission, and may also be the cause of the variable UV lines and the radio emission.

Current observations and phenomenological models of the winds and magnetospheres of the helium-strong stars suggest that these stars have mass outflows restricted to the magnetic pole regions and hot circumstellar plasma trapped in the equatorial regions of the magnetic field. A small number of helium-weak stars also show evidence for such polar outflows or magnetospheres. In addition, for some years the hottest helium-strong stars have been known to have another magnetospheric diagnostic: H α emission. Several years ago Bolton and Fullerton (U. of Toronto) used the CFHT to obtain spectacular H α observations of the prototypical helium-strong star, sigma Ori E, as well as several other members of the class. These data confirm that sigma Ori E has circumstellar material trapped in two clouds near the intersections of the star's magnetic and rotational equators.

Figure 20 illustrates the remarkable H α variability of Delta Ori C. This cool (19000 K) helium-strong star has sharp lines, a constant longitudinal magnetic field of -3.4 kG (the strongest of the entire helium-strong class) and no UV spectrum variations, so the variable nature of the H α emission is a surprise. Profile changes are obvious over time scales of an hour, and the period